Available online at www.sciencedirect.com
ScienceDirect
Optical Materials 29 (2006) 60–64
OPTICAL Materials
www.elsevier.com/locate/optmat

Characterization of metal-dielectric photonic crystals

A. Zamudio-Lara [a], J.J. Sanchez-Mondragon [a,b], M. Torres-Cisneros [c,*], J.J. Escobedo-Alatorre [a], C. Velásquez Ordoñez [a], M.A. Basurto-Pensado [a], L.A. Aguilera-Cortes [c]

[a] Center for Research on Engineering and Applied Sciences, UAEM Cuernavaca, Mor. 62160, Mexico
[b] Photonics and Optical Physics Laboratory, Optics Department, INAOE, Puebla, Pue. 72000, Mexico
[c] Optoelectronics Group, Electronics Department, FIMEE University of de Guanajuato, Salamanca, Guanajuato 36730, Mexico

Abstract

We discuss a new photonic crystal structure that arise out of including extremely thin metallic inserts in a standard dielectric photonic crystal (DPC). We had denominated dielectric-metallic photonic crystal (DMPC) to these combined structures to distinguish them from the metal dielectric photonic crystal (MDPC) with a single dielectric substrates and DPC, even when they preserve features from both, they have features of their own as a metal-dielectric structure. In this work, we numerically analyze a dielectric-metallic photonic crystal in a microsphere arrangement, characterizing the corresponding Bragg frequency and the dielectric and metallic stopgaps. In particular, we are interested in the dependence of the dielectric width σ_D and the metallic width σ_M respectively, as functions of the refraction index difference and the metal thickness d. We also discuss the structural flexibility introduced by the dielectric-metallic photonic crystal in the stopgaps pattern.

PACS: 42.70.Qs; 42.65.k; 42.70.a

Keywords: Photonics bandgaps; Metallic films; Metallic bandgap

1. Introduction

Two different approaches on photonic crystals (PC) and their photonics bandgaps (PBG) have been introduced, supported on the same basic principles of electromagnetic (EM) transmission and reflection on dielectric and metals, Both of them present fairly distinctive characteristics, the dielectric photonic crystals (DPC) is characterized by the typical stopgap [1] while the metal photonic crystals (MPC) shows a characteristic transmission peaked structure [2]. Both of them require of distinctively different scales because of the particular characteristics of the material, a DPC is referred on the wavelength dimensions while a MPC is in nanometers. The distinctively differentiated behavior of the PBG was exhaustively studied by Yablonovich et al. [2] on an array of thin metallic films of tens of nanometers thick, extending the photonic crystals concept to the metal-dielectric photonic crystal (MDPC). These structures have been generalized to more complex metallic structures, but still as inserts on a single dielectric support. On their own these metal-dielectric structures have important applications [3].

Each one of these structures, DPC and MDPC, is a basic structure, in the sense that they are based on a single process of transmission–reflection on either the dielectric or the metallic interface. In this work, we have explored a metallic dielectric photonic MDP, from thin (>10 nm) to the very thin metallic film limit (~1 nm). From our numerical results we realize that beyond the distinctive behavior of the peaked structure [2], there is a metallic stopgap

* Corresponding author. Tel.: +52 464 6480911; fax: +52 464 6472400.
E-mail addresses: jsanchez@inaoep.mx (J.J. Sanchez-Mondragon), mtorres@salamanca.ugto.mx (M. Torres-Cisneros).

0925-3467/$ - see front matter © 2006 Elsevier B.V. All rights reserved.
doi:10.1016/j.optmat.2006.03.026

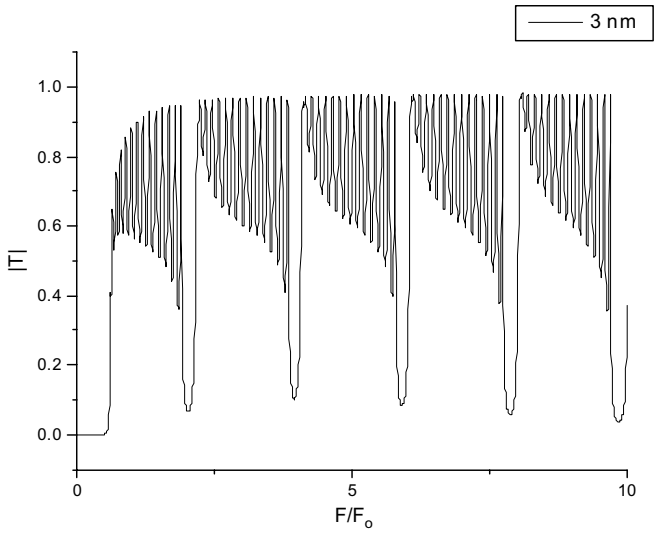

Fig. 1. Transmission in a M structure for metallic 3 nm thickness.

shown in Fig. 1, which is similar to the dielectric case. That is a new feature, that we will explore in this work, in the context of structures that integrate both features, and corresponds to a DPC as a substrate of a periodic array of metallic thin layers (DMPC).

2. Model

In thin films, previous works discuss a continuous analysis of these multiple layers structures [2], in particular taking into account the dispersion properties of these one dimensional structures [3]. In the present work, we have used the transfer matrix method which offers an effective detailed approach; layer by layer and from basic concepts. In particular, the metal case has been modeled on the Drude Model. Our analysis is based on a dielectric structure made of two dielectric D_a and D_b, with quarter wave length layers L_a and L_b, that produces a period $L = L_a + L_b$, where the refraction index for each layer are η_a and η_b, respectively. For simplicity, we have considered the presence of the metal as a small discrepancy of length d. The parameters used for metallic case [1] are $\omega_p = 1.6 \times 10^{16}$ rad (2550 Thz) and the elasticity coefficient $\delta = 1.6 \times 10^{13}$, while we used two different refraction index contrast for the dielectric materials; $\eta_b = 1.46$, $\eta_a = 3.58$ and $\eta_a = 4.58$. In our numerical analysis, we have considered 30 periods (60 dielectric layers) in most of the structures. The analyzed geometry is basically a one dimensional PC, where very thin films have been inserted in the dielectric photonic crystal DPC.

The transfer matrix method used to compute the fields inside of a DPC, in particular for two dielectric layers D_a and D_b, has been exhaustively studied [4–9]. The detailed approach introduced by the transfer matrix (M) looks at the analytical solutions layer by layer, becoming a reliable numerical experiment. Macro concepts, such as the Floquet Theorem and the Bragg wavelengths link those results with the allowed propagating and counterpropagating waves of the stack and much more complex PC structures as well. The ideal and lossless macro approach to this problem is given by the coupled mode method, given by

$$\frac{\partial E_C}{\partial z} + \frac{1}{V}\frac{\partial E_C}{\partial t} = i\theta E_P \tag{1a}$$

$$\frac{\partial E_P}{\partial z} - \frac{1}{V}\frac{\partial E_P}{\partial t} = i\theta E_C \tag{1b}$$

From the left side of Eqs. (1a) and (1b), we can recognize the terms involved in the propagation description, while the right side of both represent the coupling term with the counterpropagating wave which is denoted with a coefficient θ. The solution of these coupled equation for a DPC are well known and its transfer function describes well the reflectivity spectrum of a DPC. If we cross-substitute these equations we recover the wave equation driven by the corresponding polarization. For each mode, this equation corresponds to a harmonic oscillator equation and the introduction of a damping term in this harmonic oscillator results in an oscillation frequency modified by the decay term that in turn should translate into the Bragg frequency. This is a perturbative correction to the dielectric description, that corresponds to the simplistic introduction of a metal as just a decay source in these equations, but that misses the point of reflection as well on transmission on a very thin metal film described by the right term of these equations, and call for a correction of θ to describe faithfully both reflection–transmission processes.

We will demonstrate on an M matrix approach that the additional metal features will show up as perturbative corrections on the dielectric features, such as the dielectric stop gaps centered at the Bragg wavelength, and as non perturbative features such as additional metallic stopgaps.

3. The spherical MDPC analysis

A MDPC is obtained from a DPC where thin metal inserts are introduced. These metal inserts, in a 1D model, correspond to thin metallic films or metallic shells for a 3D case (microsphere). The 1D case has been thoroughly studied in particular regions where the metallic behavior is dominant. However, if the metallic films are still much thinner (1 nm to 10 nm), we will show that new stopgaps will appear, analogous, but without possible equivalence in the DPC. In an equivalent DPC behavior, where the bandgap properties depend on the refraction index difference of their layers, the new stop gaps depend on metal inserts thickness.

We have demonstrated previously [5] that one dimensional (1D), cylindrical (2D) and microspheres (3D) share essential Bragg features, in particular with large cores. Therefore the features discussed below are indistinctively valid for all of them. In our case, metallic thin film inserts, the Drude model claim that the permittivity for the metal

can be described as a frequency function and given by [2,3,7,9]

$$\varepsilon(\omega) = 1 - \frac{\omega_p^2}{\omega(\omega - i\gamma)} \tag{2}$$

where ε denotes the metal permittivity, ω the frequency and ω_p represents the plasma frequency. Our numerical simulations were done by using the following values $\omega_p = 1.6 \times 10^{16}\ s^{-1}$, $\gamma = 1.6 \times 10^{13}\ s^{-1}$, $f_p = 2.55 \times 10^{15}\ s^{-1}$. Metal behavior is much more complex than dielectric material behavior. We can notice that for frequencies below the plasma frequency threshold (ω_p), the refraction index will take complex values, while it will be real for frequency values above ω_p [9].

The characteristic peaked profile discussed previously by Yablanovich [2] was obtained by numerical simulation of a microsphere structure. In this structure, as we decrease the metal thickness, the metallic bandgaps arise as can be seen in Fig. 1. These bands will disappear as the metal becomes negligible, and its capability to reflect becomes reduced, recovering the dielectric bulk feature. These metallic stopgaps have characteristics which are determined by the metal layer parameters such as the metal thickness d. Our results show that the metallic stopgap is centered at a frequency that is determined by the periodicity of the metallic and the dielectric films but with a shift that depends on d. We will refer to this frequency as Bragg in analogy to the dielectric photonics crystals. Nevertheless, the metal thick value d has other consequences as the linear behavior of the stopgap width and the exponential dependence of the stopgap depth.

4. Dielectric-metal photonic crystal

The dielectric-metal photonic crystals (DMPC) is a generalization of the metal-dielectric photonic crystal (MDPC). Metal-dielectric photonic crystals are generated when thin metal inserts are inserted in a single dielectric slab, as the substrate. The dielectric-metal photonic crystals have the same structure but we have included a dielectric photonic crystal as a substrate. We realize that both features DPC and MDPC coexist and in this section we numerically characterize its dependence. Our numerical simulation was carried out for a structure of 30 periods; where each period consists of two dielectrics layers $\lambda/4$ thick and a metallic layer. The resulting structure has the form $D_aD_bMD_aD_bM\ldots D_aD_bM$, where D_a is the dielectric material a with refraction index 3.58; D_b represents the dielectric material b with refraction index 1.46 and finally, M denotes the metallic layer. The spherical structure has a Dielectric Bragg frequency of $F_0 = 192.9$ THz and a core with a radius of a 1 μm, and a refraction index of 1.5 and air as an exterior medium. Our aim is to discuss the dependence of the Bragg frequency, the width, the depth of dielectric and metallic stop gaps, on the different parameters such as: the refraction indexes and its difference (Δn), the metallic layer thick (d) and the periodicity of the metallic layer (as the dielectric correspondence is fixed).

4.1. Dielectric band

The stopgaps of a DMPC consist of two kinds, one arises from the dielectric structure of the DPC and another one from the metallic array that will correspond to an effective MDPC, and this is noticed on the dominant dependence. This fact is easily demonstrated from the transmission spectra obtained for a D_aD_bM structure show in Fig. 2, where we can recognize two metallic stop gaps on both sides (at the second and fourth Bragg frequencies), and one dielectric stopgap (central, at the third Bragg frequency). This figure also demonstrates that the variation of the refraction index difference (Δn) from 0.08 to 3, has no effect on the Bragg frequency itself but in the broadening dependence σ_{Ddm}, where its dependence can be approximated to be linear.

We define the center of the stop gap in terms of the effective Bragg frequency, and from Fig. 2, we realize that this is independent of Δn. However, we noticed that as we change the metal thickness d, the center of the gap shifts toward higher frequencies, as would be expected in a damped harmonic oscillator. Therefore, we can assume that the Bragg wavelength of a MDPC is given by

$$\omega_{BDM}^2(\eta_a, \eta_b; d) = \omega_{BD}^2(\eta_a, \eta_b) + \gamma_M^2(\eta_a, \eta_b; d) \tag{3}$$

where we can get the Bragg frequency γ_M shift as

$$\gamma_M = \sqrt{\omega_{BDM}^2 - \omega_{BD}^2} \tag{4}$$

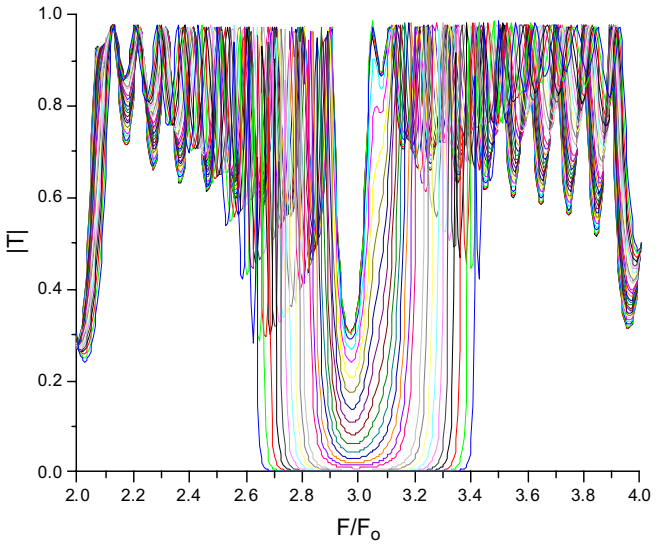

Fig. 2. Transmission spectra for a DMPC. The D_aD_bM structure shows two metallic stop gaps on the sides (second and fourth Bragg frequencies), and a central stopgap coming from the dielectric material (third Bragg frequency). Varying the refraction index difference (Δn) between 0.08 and 3 demonstrate no effect on the Bragg frequency itself but in broadening of the stop gap. The dependence of σ_{Ddm} from Δn is linear considering the fit: $\sigma_{DM} = \sigma_0 + e\Delta n - f\Delta n^2$; where $\sigma_0 = 0.15254$, $e = 0.33579$ and $f = 0.03605$.

Plotting Eq. (4) for a D_aD_bM. structure, we realize that the shifting of the Bragg frequency γ_M, is basically a linear function on the metal thickness d, as is shown in Fig. 3, with small quadratic corrections that clearly will become dominant in the domain previously explored by Yablonovich [1]. Fig. 4 shows the evolution of the stopgap thickness (σ_{Dmd}) which has a much more interesting behavior; from a small linear perturbation that initially means a reduction on the width of the stopgap, quickly sets on a quadratic increase on σ_{Dmd}.

Each line in Figs. 3 and 4 represents different refraction index difference value (Δn); 2.12 and 3.12 for (a) line and (b) line, respectively. The direct dependence of this parameter can be observed at $d = 0$ in both figures; while is negligible in γ_M (Fig. 3) is expectedly evident for σ_{Dmd} (Fig. 4). This Δn dependence can be seen from the correction behavior; which mean that the slope and the curvature in each Figure is more significant as Δn gets smaller.

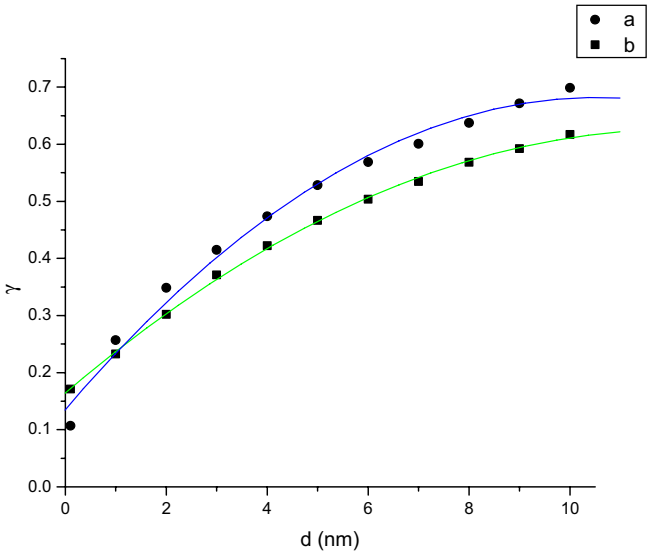

Fig. 3. Bragg frequency shifting (γ_M), from Eq. (4), as a function of the metallic film thickness d in a D_aD_bM structure. (a) $\eta_a = 3.58$ and $\eta_b = 1.46$, $\Delta n = 2.12$ and (b) $\eta_a = 4.58$ and $\eta_b = 1.46$; $\Delta n = 3.12$. The numerical fitting shows that $\gamma = \gamma_0 + bd - cd^2$ such that $c \ll b$ (a) $\gamma_0 = 0.13524$, $b = 0.10367$ and $c = 4.91 \times 10^{-3}$ and (b) $\gamma_0 = 0.16461$, $b = 0.07552$ and $c = 3.09 \times 10^{-3}$.

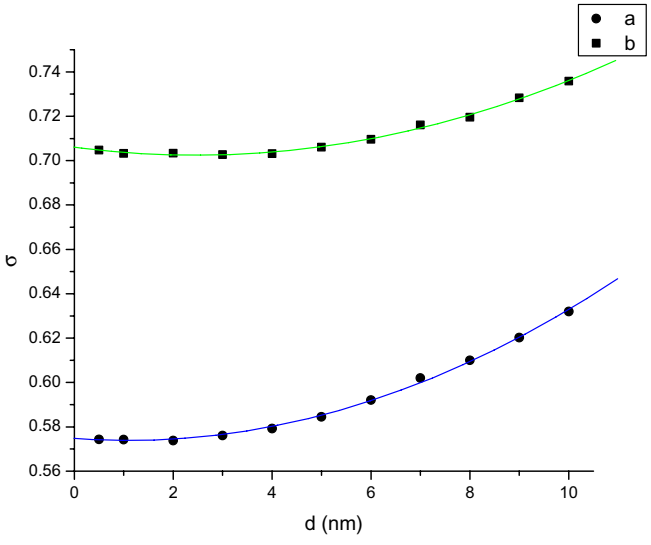

Fig. 4. σ_{Dmd} as function of the metallic width d in a D_aD_bM structure. (a) $\eta_a = 3.58$ and $\eta_b = 1.46$, $\Delta n = 2.12$ (b) $\eta_a = 4.58$ and $\eta_b = 1.46$; $\Delta n = 3.12$. The fitting is $\sigma = \sigma_0 - sd + wd^2$ for Δn constant where (a) $\sigma_0 = 0.57476$, $s = 1.62 \times 10^{-3}$, $w = 7.43944 \times 10^{-4}$ (b) $\sigma_0 = 0.70604$, $s = 2.91 \times 10^{-3}$, $w = 5.91358 \times 10^{-4}$ the minimum value occurs at $d_0 = s/2w$, that corresponds to (a) $d_0 = 1.089$ and (b) $d_0 = 2.460$.

4.2. Metallic band

One of the most interesting aspects of a DMPC is the metallic bands, that are not only dependent on the thickness and the periodicity of the metallic films, but also in a smaller degree on the dielectric features such as the refraction index difference of the DPC substrate. The most striking feature of these bands is that they occur where the DPC has transmittivity, therefore they are not perturbative effects in spite of arising from very thin metallic layers. The metallic band characterization obtained for different values of metal thickness is shown in Fig. 5, where we have considered a spherical structure with 30 periods, each one made of three layers of different materials: two dielectric layers, $\lambda_0/4$ thick and one metallic layer. The refraction indexes used are $\eta_a = 3.58$ (Si) and $\eta_b = 1.46$ (SiO_2) with thickness of 0.1082 μm and 0.2654 μm respectively, the Bragg frequency was $F_0 = 192.9$ THz. Finally, we had used metallic thick layers of $d = 0.1$ nm and $d = 3.0$ nm. A detailed glance of Fig. 5 also shows clearly evidence of the σ_{Dmd} dependence on the metal thickness d, showing that in the limit, for extremely thin metal layer, we obtain typical DPC stopgaps. We calculated this dependence to be linear for the given parameters values: $\sigma = \sigma_0 + bd + cd^2$; $\sigma_0 = 3.667 \times 10^{-2}$, $b = 4.747 \times 10^{-2}$, $c = -1.09 \times 10^{-2}$. Others d dependences of the metallic stop gap were

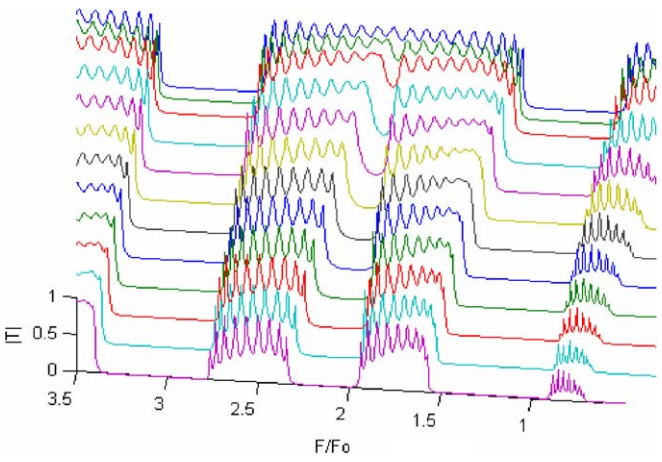

Fig. 5. Transmission spectra of a DDM structure varying thickness of a metallic film.

numerically estimated resulting in a interesting linear relation on the refraction index difference Δn ($\sigma^{D}_{BDM} = \sigma_0 + e\Delta n + f\Delta n^2$ where $\sigma_{0d} = 0.1119$, $e = -1.4445 \times 10^{-4}$, $f = 2.25 \times 10^{-3}$), and an exponential decay on the depth of the metallic bandgap ($T = T_0 e^{-d/D}$, $T_0 = 0.899$ and $D = 1.66088$).

5. Conclusions

The merging into a newer class of PC of the MDPC and the DPC, with its enormous legacy of scientific development and technological experience, opens a new space where both structures intertwined into much more complex class of structures, but still tractable on their PC parent, not only as limiting cases but in general trough mixed features. The DMPC includes conveniently joint features that allow tailoring improvements in already available devices and providing new enabling features.

The supporting structure are the DPC whose dielectric stopgaps constitute the basic frame of a new set of stopgaps that as a tunable comb are provided by the flexible metallic structure of a MDPC. We have presented the analysis of the Bragg frequency and the stopgap of this hybrid system, as a function of its dielectric and metallic nature, pointing out which features are perturbative and which are not. In particular in the last ones, we discuss the narrow metallic stopgaps, their nature but also their flexibility to create tunable stopgaps based on their metallic structure in relation to the DPC.

Acknowledgements

We would like to thank to CONACyT, University of Guanajuato and to ALFA for the funding obtained through the projects: *Electrodinámica cuántica de sistemas microestructurados* (*# 45667*), *Photonic bandgap enhanced second harmonic generation in planar lithium niobato waveguide* (*# 64/2005*) and *Images: des* ß-*Puces en Epidémiologie à la Chirurgie Assistée* (*IPECA*), respectively.

References

[1] E. Yablonovitch, K.M. Leung, Physica B 175 (1991) 81.
[2] H. Contopaganos, E. Yablonovitch, N. Alexopolus, J. Opt. Soc. Am. A 16 (9) (1999).
[3] M. Scalora, M.J. Bloemer, A.S. Pethel, J.P. Dowling, C.M. Bowden, A.S. Manka, J. Appl. Phys. 83 (5) (1998).
[4] A. Yariv, P. Yeh, Optical Waves in Crystals, Wiley, New York, 1984.
[5] A. Zamudio-Lara, J. Escobedo-Alatorre, J. Sánchez-Mondragón, M. Tecpoyotl-Torres, Opt. Mater. (27) (2005).
[6] M. Koshiba, K. Saitoh, Opt. Lett. 29 (15) (2004) 1739.
[7] A. Zamudio-Lara. Estudio de las Propiedades Electromagnéticas en una Microesfera Multicapa en el rango de Frecuencias Ópticas, Ph.D. Thesis. J. Sanchez-Mondragon (adviser). INAOE, Mexico, 2005.
[8] J. Escobedo-Alatorre, Análisis no lineal de dispositivos de alta frecuencia para su aplicación en comunicaciones, Ph.D. Thesis. J. Sanchez-Mondragon, S.V. Koshevaya and M. Tecpoyotl-Torres (advisers). INAOE, Mexico, 2005.
[9] J. Sanchez-Mondragon, A. Zamudio-Lara, J. Escobedo-Alatorre, M. Tecpoyotl-Torres, D. May-Arrioja, XLVIII CONGRESO NACIONAL SMF/XVIII REUNIÓN DE LA AMO, Guadalajara, Jalisco, Mexico, 2005.